Available online at www.sciencedirect.com
SCIENCE DIRECT®
Solid-State Electronics 48 (2004) 2013–2017
SOLID-STATE ELECTRONICS
www.elsevier.com/locate/sse

Ballistic transport at GHz frequencies in ungated HEMT structures

Sungmu Kang [a], Peter J. Burke [a,*], L.N. Pfeiffer [b], K.W. West [b]

[a] *Henry Samueli School of Engineering, Electrical Engineering and Computer Science, Integrated Nanosystems Research Facility, University of California, Irvine, CA 92697-2625, USA*
[b] *Bell Laboratories, Lucent Technologies, Murray Hill, NJ 07974, USA*

Received 10 December 2003; accepted 15 March 2004

Abstract

By measuring the ac impedance, we measure for the first time the crossover from diffusive ($\omega\tau < 1$) to ballistic ($\omega\tau > 1$) transport as a function of frequency (dc to 5 GHz) in a dc contacted 2d electron gas in the low electric field limit, where τ is the momentum scattering time. The geometry is an "ungated HEMT", meaning current flows through an ohmic contact into a 2d electron gas, laterally through the 2d electron gas, and out into a second ohmic contact; the 2d electron gas itself is not gated. At the measurement temperature (4.2 K), the low field mobility is 3.2×10^6 cm^2/V s. We also measure for the first time the frequency dependent contact impedance in this ballistic limit.

PACS: 71.10.Ca; 71.55.Ed; 72.20.Dp; 72.80.Ey; 73.23.−b; 73.40.Cg
Keywords: Ballistic transport; 2d electron gas

1. Introduction

Current generation Si MOSFETs are well described using semiclassical diffusive transport models because the gate length is generally much larger than the mean-free-path of the electrons. In very high-mobility two-dimensional electron gas (2DEG) systems at cryogenic temperatures, ballistic transport is commonly observed at low electric fields. However, at the technologically relevant high-electric field strengths prevalent in HEMT devices, diffusive transport prevails because the high-field mean-free-path is usually shorter than the gate length. Shur has presented evidence that the transit time in deep-submicron HEMTs is shorter than the scattering time [1], so that ballistic effects may be relevant there already.

Gate lengths under 10 nm are called by International Technology Roadmap for Semiconductors [2]. It is generally expected that ballistic transport effects will prevail at that length scale, and this issue has been addressed in simulations by several theory groups [3–10]. The experimental realization of ballistic Si MOSFET transistors was recently reported by Bell Labs [11]. Additionally, new devices not limited by transit time effects are also possible in this regime of operation [12]. Thus, ballistic transport in gated transistors is a timely, technologically relevant topic.

Ballistic transport means that electrons move in response to an electric field without scattering. This can be achieved in two limits: first, the device size can be made smaller than the mean-free-path. Second, the frequency of the electric field can be larger than the scattering frequency, i.e. $\omega\tau > 1$. It is the second case which we focus on, in this work. By measuring the frequency dependence of the dynamical impedance of a two-dimensional electron gas, we measure for the first time the crossover from ballistic to diffusive transport in a dc

* Corresponding author. Tel.: +1-949-824-9326; fax: +1-949-824-3732.
E-mail address: pburke@uci.edu (P.J. Burke).

0038-1101/$ - see front matter © 2004 Elsevier Ltd. All rights reserved.
doi:10.1016/j.sse.2004.05.050

contacted 2DEG as a function of frequency. Particular attention is paid to the issue of the contact resistance in the limit $\omega\tau > 1$.

2. Theory and background

At low electric fields for conductors much larger than the mean-free-path, the dc current density j_{dc} is directly proportional to the dc electric field E_{dc}, while at high-dc electric fields, the current saturates. This can be written as

$$\begin{aligned} j_{dc} &= \sigma E_{dc} \quad \text{low } E_{dc} \\ j_{dc} &= j_{sat} \quad \text{high } E_{dc} \end{aligned} \tag{1}$$

At high-frequencies and low electric fields, the ac current density j_{ac} is proportional to the ac electric field E_{ac}, i.e.

$$j_{ac} = \sigma(\omega) E_{ac} \quad \text{low } E_{ac}. \tag{2}$$

High-field ac transport is generally more complicated to treat because the scattering time is energy dependent. In this paper, we focus on measurements of $\sigma(\omega)$ in the low electric field region, at frequencies below and above the scattering frequency.

According to the Drude model, the frequency dependent conductivity is given by

$$\sigma(\omega) = \frac{ne^2\tau}{m^*} \frac{1}{1 + i\omega\tau} \tag{3}$$

where τ is the momentum scattering time. The predicted dynamical impedance for a 2DEG then contains both a real and imaginary part, and can be written as

$$Z_{2DEG}(\omega) = R_{2DEG} + i\omega L_K \tag{4}$$

where $L_K = m^*/(ne^2)$ per square is called the kinetic inductance, and $R_{2DEG} = m^*/(ne^2\tau)$ per square. In a recent paper [13] some of us measured this using capacitively contacted samples. In this work, we present the first ever measurements where the dc and microwave frequency impedance are measured simultaneously on the same sample. This allows us to directly compare the dc impedance and ac impedance. The effects of the ohmic contact impedance are also measured simultaneously for the first time.

3. Fabrication and geometry

In order to achieve the ballistic limit $\omega\tau > 1$ at GHz frequencies, we perform our experiments on high-mobility modulation doped GaAs/AlGaAs quantum wells grown by molecular beam epitaxy. The experiments are performed at 4 K. The samples used have a density of 1.1×10^{11} cm^{-2} and mobility of 3.2×10^6 cm^2/V s at 4 K according to four-terminal measurements

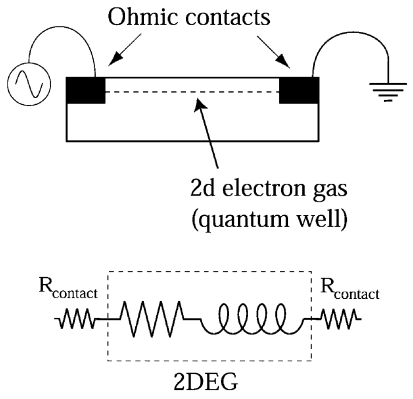

Fig. 1. Sample geometry and low field ac equivalent circuit.

done on samples from the wafer. For the measurements presented here, samples for two-terminal resistance measurements with ohmic contacts are used. The geometry of the sample (typically 500 μm × 500 μm) is defined either by direct cleaving or mesa etching. For the ohmic contact, we use evaporated Ni/Ge/Au/Ni/Au (80/270/540/140/2000 Å) metallization followed by a rapid annealing at 440 °C. The sample geometry is indicated schematically in Fig. 1 above.

4. Measurement technique

In order to characterize the two-terminal impedance of the 2DEG, we measure both the DC (13 Hz) and AC (1 MHz to 5 GHz) properties on the same sample. The DC resistance is measured using a lock-in amplifier. The AC impedance is measured by measuring the microwave reflection coefficient S_{11}, and inverting the standard reflection formula $S_{11} = (Z_{load} - 50\ \Omega)/(Z_{load} + 50\ \Omega)$. In our measurement geometry, the sample is mounted at the end of a microstrip line. A key point is that this measurement includes the ohmic contact impedance, which varies between <1 Ω and >100 Ω. We have carefully quantified the effect of the contact impedance on the microwave impedance.

5. Calibration technique and biasing

We have developed an improved calibration technique over our previous publication [13]. We measure the reflection coefficient off of a known standard (open, short, load) at 4 K. Using this data we perform a vector calibration of S_{11} to the end of the coaxial cable. We then measure the reflection off of the end of a microstrip sample mount with no sample. We find the microstrip has negligible loss up to 5 GHz, and determine the effect phase delay of the microstrip sample mount using this

method. Then, we measure the sample S_{11} by soldering it to the end of the microstrip. Using this technique we can determine the real and imaginary parts of the impedance as a function of frequency. We used two different network analyzers, an Agilent 8270 ES to cover the frequency range of 50 MHz to 5 GHz, and an Agilent 4395A to cover the frequency range of 1 MHz to 500 MHz. This allowed careful comparison of the dc resistance with the RF and microwave impedance. For the ac impedance measurements, the dc bias was zero. The incident rf amplitude was −40 dBm, which corresponds to an ac voltage of ~5 mV. These power levels were sufficient to keep the ac impedance measurements in the linear response, low field limit.

6. Results and discussion

The contact resistance to 2DEG samples in the ballistic limit ($\omega\tau > 1$) has never been studied before. In principle the contact resistance may be frequency dependent and consist of both real and imaginary parts (either capacitive or inductive). A key result of this paper is that we have measured the 2DEG plus contact resistance, and quantified the effect of the contact resistance. What we find is that the contact resistance is mostly real, and only weakly dependent on frequency. Specifically we find the following to be true

$$Z(\omega) = R_{\text{contact}} + R_{\text{2DEG}} + i\omega L_{\text{K}} \tag{5}$$

where R_{contact} is the contact resistance. In order to study whether this equation is true we have measured the two-terminal resistance of samples in three different limits: $R_{\text{2DEG}} \gg R_{\text{contact}}$, $R_{\text{2DEG}} \sim R_{\text{contact}}$, and $R_{\text{2DEG}} \ll R_{\text{contact}}$. We find Eq. (5) to be true for all three cases, as we discuss below.

The samples studied are summarized in Table 1. In Table 1, R_{dc} is the measured dc resistance. $\text{Real}(Z)_{\text{ac}}$ is the real part of the measured microwave impedance. R_{2DEG} is the calculated 2DEG impedance based on the mobility and density measured on separate samples from the same wafer and the sample geometry; R_{contact} is the measured resistance less the predicted 2DEG resistance.

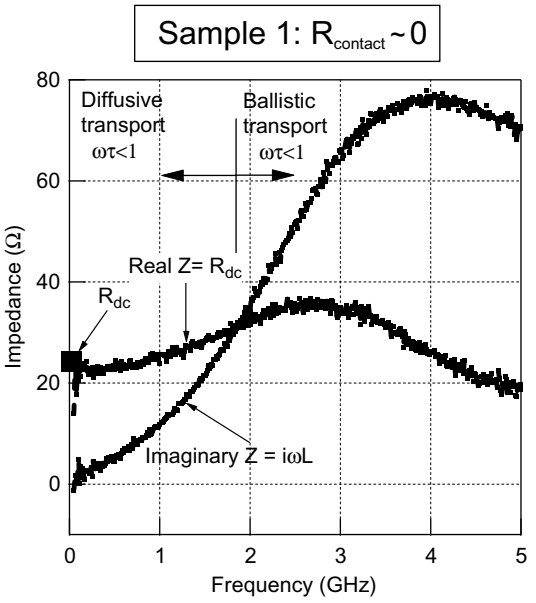

Fig. 2. Crossover from ballistic to diffusive transport vs. frequency when R_{contact} is negligible.

We first discuss the case where the contact resistance is negligible, i.e. $R_{\text{2DEG}} \gg R_{\text{contact}}$, which applies for samples 1 and 2. We plot in Fig. 2 the measured real and imaginary impedance of sample 1. According to the Drude model (Eq. (2)), if the contact impedance is negligible, then real part of the impedance is independent of frequency, and the imaginary part of the impedance is inductive, i.e. proportional to frequency. Our data support this conclusion as shown in Fig. 2. The real impedance is approximately independent of frequency, and the imaginary impedance rises linearly with frequency. The dc resistance measured for this sample (25 Ω) is equal to the real part of the impedance at GHz frequencies.

The data in Fig. 2 represent the first ever measurement of the crossover from diffusive to ballistic transport as a function of frequency in a dc contacted 2DEG. The two frequency regimes are clearly denoted on the figure. When the contact resistance is negligible, the condition $\omega\tau = 1$ (and hence the numerical value of τ)

Table 1
Summary of measured dc and ac impedance values

Sample	R_{dc} (Ω)	$\text{Real}(Z)_{\text{ac}}$ (Ω)	R_{2DEG} (Ω)	R_{contact} (Ω)	τ (ps)
1	24	25	25	<1	80
2	25	25	25	<1	80
3	62	60	24	37	80
4	100	100	17	83	80
5	250	240	34	206	–
6	22	20	13	7	80
7	45	40	30	10	80

can be determined from the measured data in this case by reading off the frequency at which $\mathrm{Re}(Z) = \mathrm{Im}(Z)$. In our experiments this crossover frequency occurs at about 1.9 GHz, implying a value of about 80 ps for τ. This value of τ so determined is reasonably consistent with the predicted value of 110 ps based on the dc measurement of the mobility on different samples from the same wafer and the relationship $\mu = e\tau/m^*$.

We next discuss the case where $R_{2\mathrm{DEG}} \sim R_{\mathrm{contact}}$, which applies to sample 3. We plot in Fig. 3 the real and imaginary impedance of sample 3. Our data show a real impedance that is independent of frequency, and an inductive imaginary impedance. The dc resistance measured for this sample (62 Ω) is equal to the real part of the impedance at GHz frequencies.

Based on the geometry of this sample we calculate that $R_{2\mathrm{DEG}} = 24\ \Omega$, implying a contact resistance (at dc) of 37 Ω. Our microwave data show that this contact resistance is independent of frequency and purely real, i.e. the contact impedance does not include any significant imaginary component. This conclusion is reflected in Eq. (5).

In Fig. 3 the crossover frequency at which $\mathrm{Re}(Z) = \mathrm{Im}(Z)$ occurs at about 4 GHz. Since $\mathrm{Re}(Z)$ includes the contact and 2DEG contribution, the frequency at which $\mathrm{Re}(Z) = \mathrm{Im}(Z)$ is not the frequency at which $\omega\tau = 1$. Rather, the condition $\omega\tau = 1$ corresponds to $\mathrm{Re}(Z_{2\mathrm{DEG}}) = \mathrm{Im}(Z)$. If we plot $\mathrm{Re}(Z_{2\mathrm{DEG}}) = \mathrm{Im}(Z)$ using the relationship $\mathrm{Re}(Z_{2\mathrm{DEG}}) = \mathrm{Re}(Z) - R_{\mathrm{contact}}$ in order to determine the frequency at which $\omega\tau = 1$, we find that occurs at 2 GHz. This gives a value for τ of 80 ps, consistent with the measured mobility and the measured crossover frequency for samples 1,2.

Finally, we discuss the case where $R_{2\mathrm{DEG}} \ll R_{\mathrm{contact}}$, which applies to samples 4 and 5. For both of these samples, the calculated 2DEG resistance based on the mobility and density measured on separate samples from the same wafer and the sample geometry is much less than the measured dc resistance. Thus, the contact resistance at dc is much larger than the 2DEG resistance. We find experimentally that, up to 5 GHz, the real part of the measured impedance is equal to the dc impedance. Thus the contact resistance is only weakly dependent on frequency, if at all. Additionally, the imaginary impedance for these two samples is inductive, consistent with the expected 2DEG impedance.

All of the data presented so far have been in the dark. We have also carried out the same measurements on the samples after illumination with a red LED. Generally we find that the resistance goes down, the inductance goes down, and the mobility (determined from the frequency at which $\mathrm{Re}(Z_{2\mathrm{DEG}}) = \mathrm{Im}(Z)$) goes up. This is consistent with well-known tendencies of these high-mobility samples to have higher mobility and density after illumination. In addition, we find that the contact impedance is real and frequency independent after illumination with an LED, as it is before illumination.

While we have focused on low electric field transport so far, we plot in Fig. 4 the current–voltage curves for the 7 devices measured to higher electric fields. The sample lengths were ~1 mm in length. The saturation velocity is clearly visible at voltages ~1 V. Therefore, the ac voltage of ~5 mV used in our ac impedance mea-

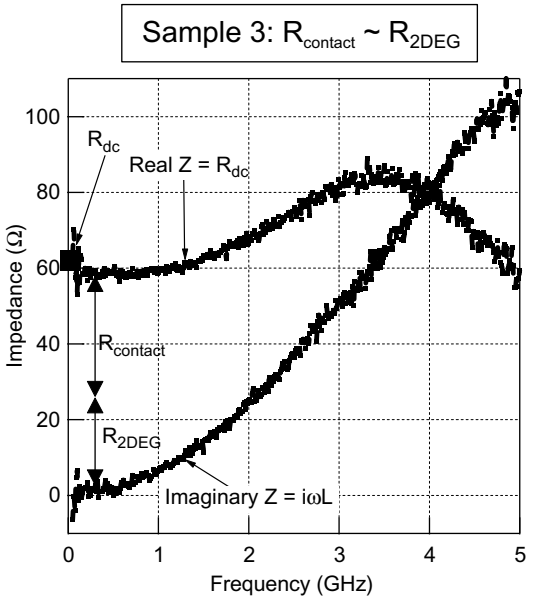

Fig. 3. Crossover from ballistic to diffusive transport as a function of frequency when R_{contact} is comparable to $R_{2\mathrm{EG}}$.

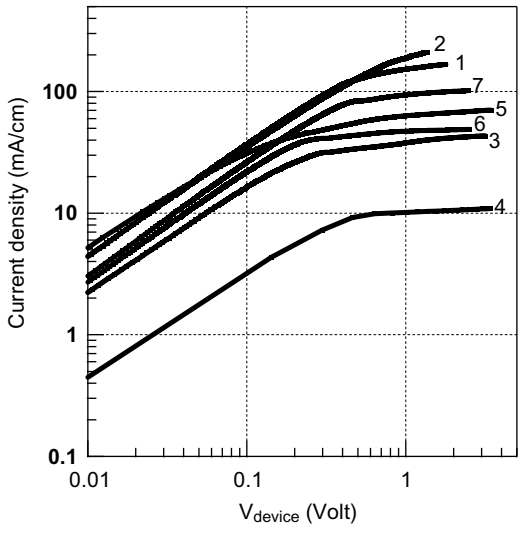

Fig. 4. Current–voltage curves for the samples measure. Each sample has a different contact resistance and number of squares, hence different I–V curve. The sample numbering scheme follows Table 1.

surements is clearly in the linear response, low field regime.

7. Conclusions

In conclusion, we have measured for the first time the crossover from diffusive ($\omega\tau < 1$) to ballistic ($\omega\tau > 1$) transport in a dc contacted 2DEG. In cases where the contact impedance is significant compared to the 2DEG impedance, we find that even in the ballistic limit for the 2DEG, the contact impedance is still real, independent of frequency, and equal to the dc measured value. This is the first experimental result on the contact impedance for samples in the ballistic limit. While this result is not surprising, it cannot be predicted from first principles because the physics of electrical contacts in this limit is not well understood. Thus the value must be determined experimentally, as we have done.

This work lays the foundation for future work on ballistic devices on both the spatial and frequency domain, i.e. devices shorter than the mean-free-path which operate at frequencies higher than the scattering frequency. This is an unexplored but technologically increasingly important regime of device operation.

Acknowledgements

This work was supported by the National Science Foundation, Office of Naval Research, Army Research Office, DARPA, U.C. SMART, and TRW.

References

[1] Shur MS. Low ballistic mobility in submicron HEMTs. IEEE Electron Dev Lett 2002;23(9):511–3.
[2] http://public.itrs.net/.
[3] Pikus FG, Likharev KK. Nanoscale field-effect transistors: an ultimate size analysis. Appl Phys Lett 1997;71(25):3661–3.
[4] Naveh Y, Likharev KK. Modeling of 10-nm-scale ballistic MOSFETs. IEEE Electron Dev Lett 2000;21(5):242–4.
[5] Lundstrom M. Elementary scattering theory of the Si MOSFET. IEEE Electron Dev Lett 1997;18(7):361–3.
[6] Datta S, Assad F, Lundstrom M. The silicon MOSFET from a transmission viewpoint. Superlattices Microstruct 1998;23(3/4):771–80.
[7] Assad F, Ren Z, Vasileska D, Datta S, Lundstrom S. On the performance limits for Si MOSFETs: a theoretical study. IEEE Trans Electron Dev 2000;47(1):232–40.
[8] Lundstrom M, Ren Z. Essential physics of carrier transport in nanoscale MOSFETs. IEEE Trans Electron Dev 2002;49(1):133–41.
[9] Natori K. Ballistic metal-oxide-semiconductor field effect transistor. J Appl Physics 1994;76(8):4879–90.
[10] Natori K. Scaling limit of he MOS transistor—a ballistic MOSFET. IEICE Trans Electron 2001;E84-C(8):1029–36.
[11] Timp G, Bude J, Bourdelle K, Garno J, Ghetti A, Gossmann H, et al. The ballistic nano-transistor. IEDM Tech Dig 1999:55–8.
[12] Dyakonov M, Shur M. Detection mixing and frequency multiplication of terahertz radiation by two-dimensional electronic fluid. IEEE Trans Electron Dev 1996;43(3):380–7.
[13] Burke PJ, Spielman IB, Eisstein JP, Pfeiffer LN, West KW. High frequency conductivity of the high-mobility two-dimensional electron gas. Appl Phys Lett 2000;76(6):745–7.